Amino Acids (2013) 44:473–480
DOI 10.1007/s00726-012-1357-0

ORIGINAL ARTICLE

Altering the Tat-derived peptide bioactivity landscape by changing the arginine side chain length

Cheng-Hsun Wu · Yi-Ping Chen · Chung-Yuan Mou · Richard P. Cheng

Received: 12 April 2012 / Accepted: 28 June 2012 / Published online: 21 July 2012

Abstract Mutations of proteins with dual activities that lead to enhancement of one activity are frequently accompanied by attenuation of the other activity. However, this mutational negative trade-off phenomenon typically only involves the canonical 20 amino acids. To test the effect of non-canonical amino acids on the negative trade-off phenomenon, two bioactivities of HIV-1 Tat-derived peptides were monitored upon changing the Arg side chain length. In contrast to the expected mutational negative trade-off, shortening Arg by one methylene resulted in both higher TAR RNA binding specificity and higher cellular uptake. These results suggest that introducing previously unexploited building blocks, even if the difference is only one methylene, can alter the peptide bioactivity landscape leading to the enhancement of multiple bioactivities.

Keywords Arginine · Side chain length · Cellular uptake · RNA recognition

Abbreviations

Agb	(*S*)-2-Amino-4-guanidinobutyric acid
Agh	(*S*)-2-Amino-6-guanidinohexanoic acid
Arg	Arginine
βAla	Beta-alanine
BIV	Bovine immunodeficiency virus
CD4	Cluster of differentiation 4
CHO Cells	Chinese hamster ovary cells
EDTA	Ethylenediaminetetraacetic acid
EMSA	Electrophoretic mobility shift assay
HIV-1	Human immunodeficiency virus type 1
HPLC	High performance liquid chromatography
K_D	Dissociation constant
MALDI-TOF	Matrix-assisted laser desorption ionization time-of-flight
MS	Mass spectrometry
NMR	Nuclear magnetic resonance spectroscopy
PBS	Phosphate buffered saline
PI	Propidium iodide
Poly(dI-dC)	Poly(2′-deoxyinosinic-2′-deoxycytidylic) acid
R	Fluorescence anisotropy
RNA	Ribonucleic acid
TAR	Transactivator response element
Tat	Transactivator of transcription
Tris	Tris(hydroxymethyl)aminomethane
tRNA	Transfer ribonucleic acid

Electronic supplementary material The online version of this article (doi:10.1007/s00726-012-1357-0) contains supplementary material, which is available to authorized users.

C.-H. Wu · Y.-P. Chen · C.-Y. Mou · R. P. Cheng (✉)
Department of Chemistry, National Taiwan University, Taipei 10617, Taiwan
e-mail: rpcheng@ntu.edu.tw

Introduction

Protein neofunctionalization occurs by accumulating mutations that enhance a secondary latent promiscuous function (Zhang 2003; Khersonsky et al. 2006; Soskine and Tawfik 2010; Tawfik 2010). Many of these mutations that facilitate the emergence of the new function are accompanied by weak but quantifiable negative trade-offs of the existing native function (Aharoni et al. 2005; Vick et al. 2005; Khersonsky et al. 2006; McLoughlin and Copley 2008; Levin et al. 2009; Soskine and Tawfik 2010). For evolution at this single protein level, multi-function or functionally generalized proteins serve as evolutionary

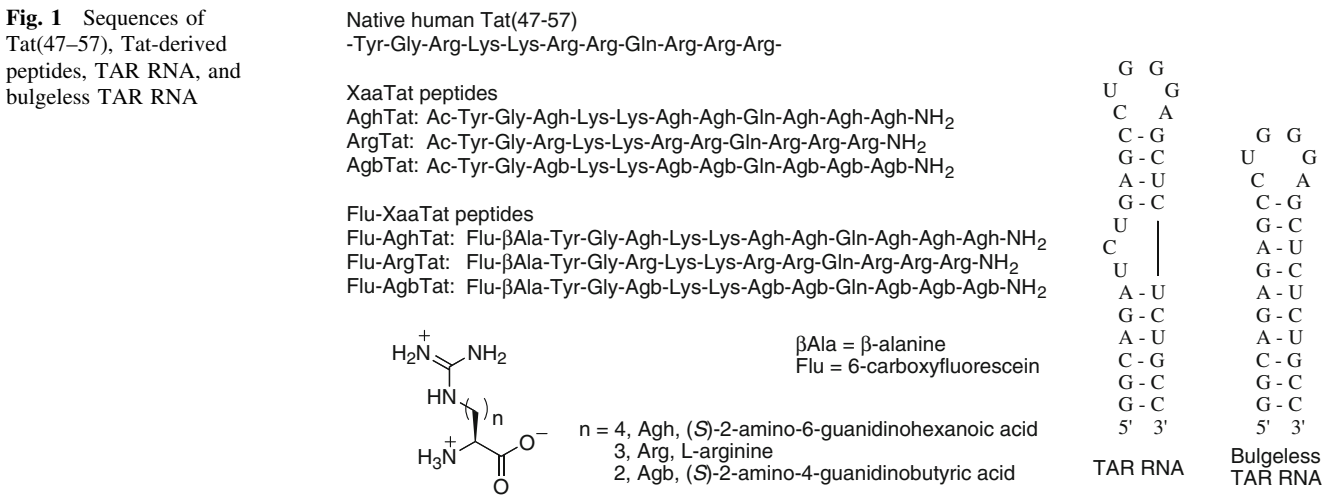

Fig. 1 Sequences of Tat(47–57), Tat-derived peptides, TAR RNA, and bulgeless TAR RNA

intermediates between the protein specialized in the existing function and the protein specialized in the new function (McLoughlin and Copley 2008). Proteins with dual activity could be an intended functionally generalized protein or a specialized protein with a secondary latent function, depending on the extent of evolution of the secondary activity (McLoughlin and Copley 2008). Importantly, mutations that further enhance either activity should lead to the attenuation of the other due to mutational negative trade-offs (Aharoni et al. 2005; Vick et al. 2005; Khersonsky et al. 2006; McLoughlin and Copley 2008; Levin et al. 2009; Soskine and Tawfik 2010). However, these naturally occurring mutations are limited to the 20 canonical amino acids. In this study, we challenge the mutational negative trade-off phenomenon with non-canonical amino acids to potentially alter the peptide bioactivity landscape.

The 11-amino acid basic region of HIV-1 Tat protein (human immunodeficiency virus type 1 transactivator of transcription protein, residues 47–57), Tat(47–57) (Fig. 1), binds to the transactivator response element (TAR) RNA (Cordingley et al. 1990; Weeks et al. 1990), and is responsible for cell penetration (Vives et al. 1997; Richard et al. 2003). The Tat–TAR interaction is crucial for HIV proliferation (Cullen 1991; Stevens et al. 2006), whereas the cell penetration capability of Tat is important for inducing viral proliferation in infected neighboring cells (Ensoli et al. 1993) and inducing apoptosis of nearby healthy immune cells (Berman et al. 2007; Misumi et al. 2004). However, Tat(47–57) binds the bulge-deleted TAR RNA with higher affinity compared to the native bulge-containing TAR RNA (Gelman et al. 2003). Furthermore, Arg_8 and Arg_9 peptides are more effective in cell penetration compared to Tat(47–57) (Wender et al. 2000). Also, Arg_9 binds TAR RNA with slightly lower specificity compared to Tat(47–57) based on gel shift data (Calnan et al. 1991b). As such, Tat(47–57) most likely represents a balance between specific TAR RNA recognition and cell penetration.

The six Arg residues in Tat(47–57) are critical for both specific TAR RNA recognition (Calnan et al. 1991a) and cell penetration (Wender et al. 2000), making Tat(47–57) an ideal system to explore the effect of introducing non-canonical Arg analogs with varying side chain length on the peptide bioactivity landscape. Accordingly, we report the incorporation of non-canonical arginine analogs with different side chain lengths, resulting in the simultaneous enhancement of the two bioactivities (i.e., specific RNA binding and cell penetration) for the basic region of the Tat protein. This suggests that introducing previously inaccessible building blocks, even if the difference is only the number of methylenes, can alter the original molecular bioactivity landscape.

Materials and methods

Peptide synthesis

The peptides were synthesized by solid-phase peptide synthesis using Fmoc-based chemistry (Atherton et al. 1978; Cheng et al. 2011). (*S*)-2-Amino-6-guanidinohexanoic acid (Agh)-containing peptides were synthesized using Fmoc-Agh$(Boc)_2$-OH following standard protocols. (*S*)-2-Amino-6-guanidinobutyric acid (Agb)-containing peptides were synthesized by solid-phase guanidinylation (Cheng et al. 2011). After cleavage, the peptides were purified by reverse-phase HPLC and confirmed by MALDI-TOF MS.

Fluorescence anisotropy experiments

Fluorescein-labeled RNA (25 nM) was titrated with peptide in 50 mM Tris–HCl, pH 7.4, 20 mM KCl, and 0.02 % Tween20 at room temperature, and monitored by fluorescence spectroscopy (Gelman et al. 2003). The fluorescence intensity with various combinations of orientations for the

excitation polarizer and emission polarizer was measured to derive the fluorescence anisotropy (R) for each addition (Lakowicz 1999). The apparent dissociation constant for the peptide-RNA complex was derived by fitting the anisotropy data assuming a 1:1 peptide-RNA stoichiometry (Puglisi et al. 1995; Gelman et al. 2003) using the full quadratic equation (Eq. 1).

$$R = R_{\text{unbound}} + \frac{\left([\text{RNA}]_{\text{total}}+[\text{peptide}]_{\text{total}}+K_{\text{D}} - \sqrt{\left([\text{RNA}]_{\text{total}}+[\text{peptide}]_{\text{total}}+K_{\text{D}}\right)^2-4[\text{RNA}]_{\text{total}}\cdot[\text{peptide}]_{\text{total}}}\right)}{2[\text{RNA}]_{\text{total}}}(R_{\text{bound}} - R_{\text{unbound}}) \quad (1)$$

R is the fluorescence anisotropy observed at the total peptide concentration $[\text{peptide}]_{\text{total}}$, R_{unbound} is the fluorescence anisotropy of unbound RNA, R_{bound} is the fluorescence anisotropy of RNA bound to peptide, $[\text{RNA}]_{\text{total}}$ is the total RNA concentration (including unbound RNA and bound RNA), $[\text{peptide}]_{\text{total}}$ is the total peptide concentration (including unbound peptide and bound peptide), and K_{D} is the apparent dissociation constant for the RNA-peptide complex.

Electrophoretic mobility shift assay

Fluorescein-labeled RNA (100 nM) and peptide (at various concentrations) were incubated in pH 7.4 buffer (10 μL) containing Tris–HCl (50 mM), KCl (50 mM), poly(dI-dC) (10 μg/mL), 2 % glycerol, and Triton X-100 (0.05 %) at room temperature. The samples were analyzed by loading into 12 % native polyacrylamide gels in 0.5 % TB buffer and electrophoresis was performed with 140 V at room temperature. Bands corresponding to the free and bound RNA were used to determine the fraction bound RNA. The fraction bound RNA data were used to globally derive the apparent dissociation constants assuming a 1:1 binding stoichiometry (Puglisi et al. 1995; Gelman et al. 2003) using the full quadratic equation (Eq. 2).

$$\text{Fraction bound RNA} = \frac{\left([\text{RNA}]_{\text{total}}+[\text{peptide}]_{\text{total}}+K_{\text{D}} - \sqrt{\left([\text{RNA}]_{\text{total}}+[\text{peptide}]_{\text{total}}+K_{\text{D}}\right)^2-4[\text{RNA}]_{\text{total}}\cdot[\text{Peptide}]_{\text{total}}}\right)}{2[\text{RNA}]_{\text{total}}} \quad (2)$$

where $[\text{RNA}]_{\text{total}}$ is the total RNA concentration (including unbound RNA and bound RNA), $[\text{peptide}]_{\text{total}}$ is the total peptide concentration (including unbound peptide and bound peptide, and K_{D} is the apparent dissociation constant for the RNA-peptide complex.

Cellular uptake assay

Jurkat cells (8×10^5) were incubated with the peptides at various concentrations (7, 30, 60, and 120 μM) at 37 °C with 5 % CO_2 for 15 min. The cells were then incubated with 0.05 % trypsin/EDTA in PBS for 5 min to remove the peptides which adhered to the cell surface rather than entered into the cell (Richard et al. 2003). Propidium iodide (PI) was added to all samples to stain the dead cells but should not stain the live cells. The cells were then transferred into the flow tube and analyzed by flow cytometry (FACScan, Becton–Dickinson Bioscience). The minimum PI fluorescence intensity for the dead control cells (which were terminated by adding Triton X-100) treated with PI was set as the threshold value. The mean 6-carboxyfluorescein fluorescence intensity for 10,000 live cells (with appropriate forward scatter and side scatter values, and below the PI fluorescence threshold) was determined for each experiment. Each experiment was independently repeated at least three times.

Results

Peptide design

The native Tat(47–57) was capped at both termini to give peptide ArgTat (Fig. 1). All six Arg residues were replaced with Agh (one methylene longer than Arg) and Agb (one methylene shorter than Arg) to give peptides AghTat and AgbTat (Fig. 1), respectively. To enable the detection of cellular uptake, the peptides were capped with 6-carboxyfluorescein at the N-terminus with an intervening βAla

(Gelman et al. 2003) to give the Flu-XaaTat peptides (Fig. 1).

RNA binding affinity determined by fluorescence anisotropy

The effect of Arg side chain length on RNA binding by XaaTat peptides was investigated by fluorescence anisotropy (Table 1). The HIV TAR RNA and the corresponding bulge-deleted TAR were labeled with fluorescein at the 3′-terminus to enable these experiments. The fluorescence anisotropy of fluorescein-labeled RNA (25 nM) was monitored upon adding varying amounts of peptide (Figs. S1, S2). The apparent dissociation constants (K_D) were derived from the experimental data assuming a 1:1 binding stoichiometry using the full quadratic equation (Gelman et al. 2003) (Table 1), because BIV (bovine immunodeficiency virus) Tat peptide binds BIV TAR RNA with such a ratio as shown in the structures derived from NMR data (Puglisi et al. 1995).

All three peptides bound TAR RNA with sub-micromolar affinity (Table 1). Since the apparent K_D for the peptide-TAR RNA complexes did not vary with Arg side chain length, the guanidinium group alone may be sufficient for TAR RNA binding. Towards binding the corresponding bulge-deleted TAR RNA, the apparent K_D for the peptide-RNA complexes decreased with decreasing side chain length (Table 1). Importantly, the binding affinity was higher for the bulge-containing TAR compared to the bulgeless RNA, regardless of side chain length.

Table 1 Apparent dissociation constants for the binding of XaaTat (Xaa=Agh, Arg and Agb) peptides with HIV TAR-related RNA in the absence and presence of poly(dI-dC)

Peptide	Apparent K_D (nM)[a]			
	RNA alone		RNA with poly(dI-dC)	
	TAR[b]	Bulgeless TAR[b]	TAR with poly(dI-dC)[c]	Bulgeless TAR with poly(dI-dC)[c]
AghTat	36 ± 9	99 ± 8	450 ± 40	ND[d]
ArgTat	25 ± 3	75 ± 8	67 ± 19	7000 ± 1000
AgbTat	32 ± 9	51 ± 4	31 ± 9	2400 ± 200

[a] The apparent dissociation constants were derived from the experimental data assuming a 1:1 binding stoichiometry

[b] Values determined by fluorescence anisotropy experiments. The experiments were performed by titrating the peptide into 25 nM fluorescein-labeled HIV TAR RNA or corresponding buldgeless TAR RNA

[c] Values determined by electrophoretic mobility shift assays (EMSA). The assays were performed with 100 nM fluorescein-labeled HIV TAR RNA or corresponding buldgeless TAR RNA, varying amounts of peptide, in the presence of 10 μg/mL poly(dI-dC)

[d] No binding was observed even in the presence of 3,000 nM peptide

RNA binding specificity determined by electrophoretic mobility shift assays

Many negatively charged entities exist in the cell, which may bind non-specifically to the positively charged peptides. Accordingly, to determine the specific binding of the peptides to the bulge-containing TAR and the corresponding bulgeless RNA, electrophoretic mobility shift assays (EMSA) were performed in the presence of competing negatively charged poly(dI-dC) (Zondlo and Schepartz 1999) to obtain the apparent K_D with attenuated nonspecific binding, i.e., specificity (Figs. 2, 3; Fig. S3; Table 1). The affinity of ArgTat for TAR RNA was somewhat affected by the presence of poly-anionic poly(dI-dC), whereas the affinity of AghTat was significantly reduced upon adding poly(dI-dC). Surprisingly, the affinity of AgbTat for TAR RNA was not affected by the presence of poly(dI-dC); the affinity of AgbTat for TAR

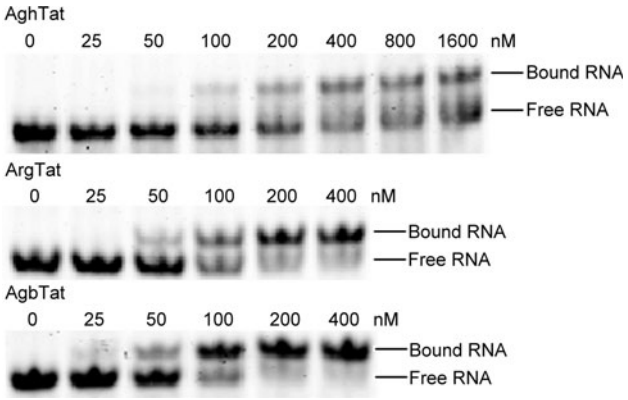

Fig. 2 Gel images of electrophoretic mobility shift assays for XaaTat peptides with 100 nM fluorescein-labeled HIV TAR RNA in the presence of 10 μg/mL poly(dI-dC)

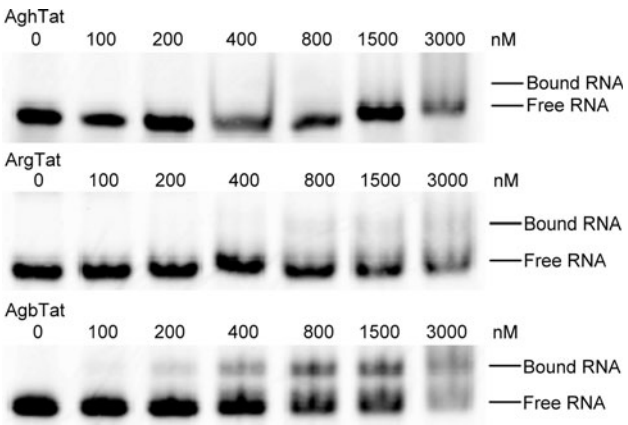

Fig. 3 Gel images of electrophoretic mobility shift assays for XaaTat peptides with 100 nM fluorescein-labeled bulge-deleted HIV TAR RNA in the presence of 10 μg/mL poly(dI-dC)

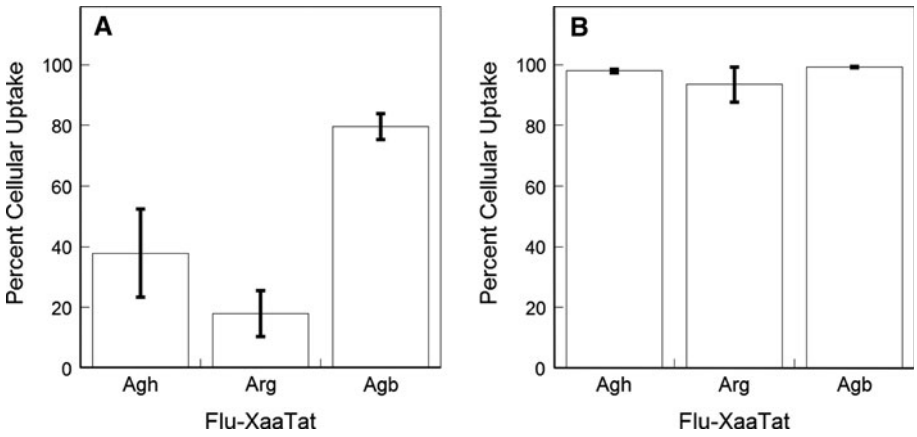

Fig. 4 Flow cytometry results for cellular uptake of Flu-XaaTat peptides into Jurkat cells in the presence of fetal bovine serum at 37 °C. Cellular uptake upon incubation (%) with 7 μM (**a**) and 30 μM (**b**) peptide for 15 min based on a strict threshold (Figs. S8, S9)

RNA in the absence of poly(dI-dC) determined by EMSA ($K_D = 36 \pm 10$ nM; Fig. S4) was essentially the same as that determined by the fluorescence anisotropy experiments ($K_D = 32 \pm 9$ nM; Table 1). Furthermore, the binding affinity in the presence of bulk tRNA as the competing negatively charged species showed the same apparent affinity trend for TAR RNA: AgbTat > ArgTat > AghTat (Figs. S5, S6). In contrast, the affinity of the peptides for the corresponding bulgeless RNA were all greatly attenuated upon adding poly(dI-dC) (Fig. 3; Table 1), indicating that non-specific electrostatic interactions are the main reason for the binding of the peptides for this closely related RNA species. These results suggest that altering the Arg side chain length does not affect the affinity between Tat and TAR, but affects specificity. In particular, shortening the Arg side chain length to Agb increases the binding specificity between Tat and TAR RNA, perhaps by limiting the motion of the guanidinium group or by providing optimal distances between guanidinium groups to interact with RNA.

Cellular uptake experiments

Cellular uptake experiments were performed on Jurkat cells, because these cells are a CD4+ helper T cell cancer cell line, and CD4+ helper T cells are the target of HIV-1. Jurkat cells were incubated separately with various concentrations (7, 30, 60, and 120 μM) of Flu-XaaTat for 15 min at 37 °C in the presence of fetal bovine serum, and then treated with trypsin to remove cell-surface bound peptide (Richard et al. 2003). Cellular uptake was visualized qualitatively using fluorescence microscopy (Fig. S7), showing obvious uptake for all three peptides.

Cellular uptake was then investigated quantitatively using flow cytometry (Fig. 4; Figs. S8, S9); only live cells were included in these studies. Using a strict threshold, more than 70 % of the cells showed uptake upon shortening the Arg side chain length by one methylene to Agb and incubating cells with 7 μM peptide (Fig. 4a; Fig. S8). Importantly, nearly all cells exhibited peptide uptake upon raising the peptide concentration to 30 μM regardless of side chain length (Fig. 4b; Fig. S9).

The amount of peptide uptake into the cells was also determined by flow cytometry. Incubating with 7 μM peptide, Flu-AgbTat exhibited 3 times higher uptake into cells compared to Flu-ArgTat and Flu-AghTat (Fig. 5a; Fig. S8). This exceptional uptake of the Agb-containing peptide was also present at higher peptide concentrations (Fig. 5b). Interestingly, Flu-AghTat exhibited slightly more cellular uptake compared to Flu-ArgTat at concentrations higher than 7 μM (Fig. 5b), consistent with a literature report on Arg_7 and Agh_7 uptake into Jurkat cells (Mitchell et al. 2000). However, the results on Flu-AgbTat (at all concentrations studied) significantly differed from the published results on Agb_7 (Mitchell et al. 2000), suggesting that the Tat(47–57) system is distinctly different from poly-arginine peptides (Mitchell et al. 2000). Interestingly, preliminary studies showed that the uptake of Flu-XaaTat peptides did not decrease upon lowering the temperature from 37 to 4 °C (Fig. S10), suggesting uptake through non-endocytotic mechanisms (Mitchell et al. 2000; Thoren et al. 2003). Importantly, altering the Arg side chain length in Tat(47–57) increased the cellular uptake of the peptides, especially when the Arg side chain length was shortened by one methylene to Agb.

Discussion

Our studies have revealed that increasing the Arg side chain length in the Tat-derived peptide greatly diminished the specificity for binding TAR RNA, with very slight effect on cell penetration. In contrast, decreasing the Arg side chain length in the same Tat-derived peptide enhanced both TAR RNA binding specificity and cell penetration capabilities. Among these Arg analogs with varying side chain length (Fig. 1), Agh has the longest side chain with the most hydrophobicity and conformational flexibility,

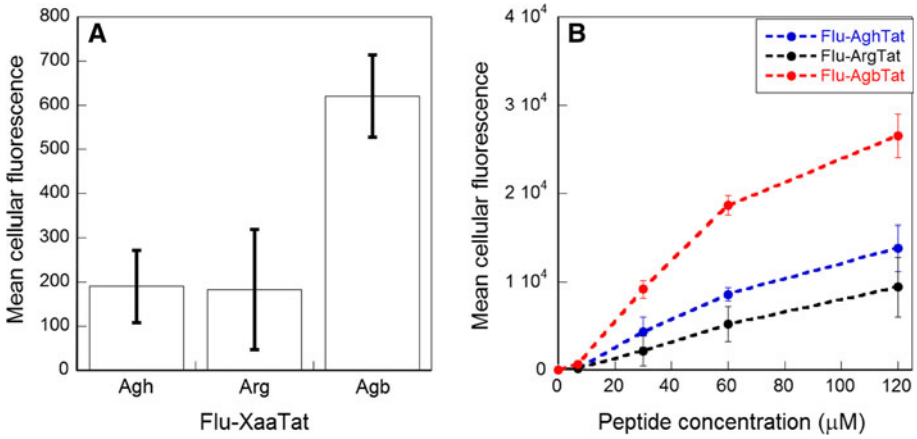

Fig. 5 Flow cytometry results for cellular uptake of Flu-XaaTat peptides into Jurkat cells in the presence of fetal bovine serum at 37 °C. Mean cellular fluorescence upon incubation with 7 μM peptide (**a**) and various peptide concentrations (**b**) for 15 min

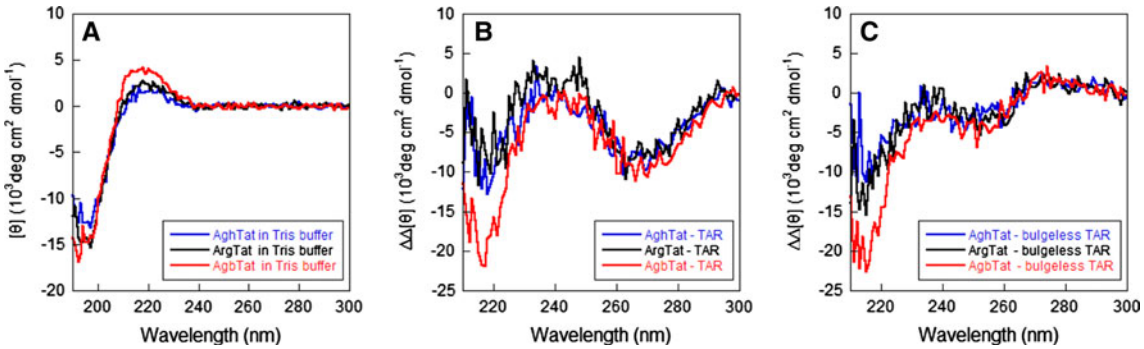

Fig. 6 **a** CD spectra of XaaTat peptides in 10 mM Tris at pH 7. **b** Difference CD spectra obtained by subtracting the TAR- and peptide-only spectra from the XaaTat-TAR complex spectrum in 10 mM of potassium phosphate and 10 mM KCl at pH 7.5. **c** Difference CD spectra obtained by subtracting the bulgeless TAR- and peptide-only spectra from the XaaTat-bulgeless TAR complex spectrum in 10 mM of potassium phosphate and 10 mM KCl at pH 7.5. The spectra are reported in mean residue ellipticity, normalized to the number of backbone amide bonds in the peptide XaaTat

presenting the guanidinium group with the most possible number of orientations. Furthermore, the Agb side chain has the shortest side chain with the least hydrophobicity and conformational flexibility. It appears that increasing the Arg side chain length to Agh lowers the TAR RNA binding specificity most likely because the side chain guanidinium groups are able to adopt orientations suitable for binding a plethora of nucleic acid structures. In contrast, shortening the Arg side chain length to Agb increases the TAR RNA binding specificity by restricting the possible three-dimensional presentations of the guanidinium groups while maintaining the proper arrangement for TAR RNA binding.

Understanding the detailed structural basis for the difference in RNA binding upon lengthening and shortening the Arg side chain length would require knowledge in the structural effect of introducing these Arg analogs on both the Tat-derived peptide itself and the Tat-TAR structure. There have been some limited studies on the structural consequence of incorporating these Arg analogs in helical peptides. In coiled coils, the Arg side chain length could be shortened to Agb without affecting stability (Kennan and Diss 2008). In monomeric Ala-based peptides, Arg was the most optimal for helix propagation (Cheng et al. 2011), whereas Agh was the most suitable for C-capping (Cheng et al. 2011). However, the structure of Tat(47–57) bound to HIV-1 TAR RNA remains unknown, hampering further analysis without this structural information.

The secondary structure of the XaaTat peptides alone was investigated by circular dichroism spectroscopy (CD) to perhaps understand the difference in bioactivity of these peptides. The CD spectra of the peptides were acquired at pH 7 (Fig. 6a). The CD of ArgTat is consistent with literature reports on the natural Tat peptide, which exhibits no structure (Mucha et al. 1998) or some evidences for the poly(proline) II helix in aqueous solutions (Ruzza et al. 2004). The peptides AghTat and ArgTat showed essentially identical CD spectra, whereas AgbTat showed a slightly more positive signal around 205–230 nm (Fig. 6a).

The CD spectral changes upon forming the peptide-RNA complexes were also obtained to perhaps understand

the difference in RNA binding specificity for these peptides (Fig. 6b, c; Figs. S11, S12). The spectral changes involving TAR RNA were similar to those previously reported for the native Tat-derived peptide (Calnan et al. 1991a; Long and Crothers 1995). Furthermore, peptide-RNA complex formation induced a more negative CD signal at 260 nm for TAR RNA compared to bulgeless TAR, as mentioned in an earlier report (Calnan et al. 1991a). Interestingly, AgbTat induced a more negative signal around 220 nm compared to ArgTat and AghTat. The slightly different CD signature for AgbTat alone and complexed with RNA compared to the other two peptides may be related to the enhanced TAR RNA binding specificity.

Increased uptake has been previously shown upon lengthening the guanidinium-bearing side chain for peptoid homo-oligomers (Wender et al. 2000). Similarly, the amount of uptake of poly-arginine peptides increased with increasing side chain length, following the trend: $Agh_7 > Arg_7 > Agb_7$ (Mitchell et al. 2000). In contrast, our results on Tat-derived peptides showed the most efficient uptake for the peptide with the shortest side chain AgbTat. The enhanced uptake of the AgbTat may be due to the Agb side chain length for presenting the guanidinium groups to enable favorable interaction with cell-surface heparan sulfate, which has been shown to be important for Arg_9 uptake into CHO cells (Elson-Schwab et al. 2007), or other cell-surface negatively charged entities (Wender et al. 2008). Since the details of the distribution of the positive charges appear to be an important factor in heparan sulfate binding and thus cellular uptake (Chao et al. 2010), changing the Arg side chain length may affect the interaction with cell-surface heparan sulfate and thereby affect cellular uptake. Furthermore, the presence of the two positively charged Lys residues and the intervening Gln residue in the Tat-derived peptides provide a unique distribution of the positively charged functionalities. As such, it is not surprising that the Tat-derived peptides behave differently compared to either the poly-arginine system or the peptoid homo-oligomer system.

Peptides derived from the basic region of Tat can inhibit Tat-dependent viral particle production at 50 μM (Choudhury et al. 1998; Mi et al. 2005), showing promise as anti-HIV therapeutics. Furthermore, peptides containing Arg analogs with varying side chain length show higher protease resistance compared to the corresponding Arg peptides (Izdebski et al. 2004). This suggests that AgbTat may be suitable for drug delivery or anti-HIV therapeutics. Preliminary studies on Jurkat cells showed minimal cytotoxicity upon exposure to 120 μM of the Agb-containing peptide for 4 h at 37 °C (Fig. S13). Further studies on AgbTat will be necessary for developing anti-HIV therapeutics or drug delivery applications.

Conclusion

Native Tat(47–57) exhibits two distinct biological functions including specific TAR RNA recognition and cell penetration. Tat(47–57) appears to represent a balance between these two bioactivities. Since mutational negative trade-off occurs in protein neofunctionalization (Aharoni et al. 2005; Vick et al. 2005; Khersonsky et al. 2006; McLoughlin and Copley 2008; Levin et al. 2009; Soskine and Tawfik 2010), further improvement of one activity should lead to deterioration of the other. In sharp contrast, our results showed that shortening Arg by one methylene to Agb in Tat-derived peptides resulted in enhancement of both RNA binding specificity and cellular uptake. This suggests that introducing similar but previously unexploited building blocks (even if the difference is only the number of side chain methylenes) can alter the bioactivity landscape, leading to simultaneous enhancement of both activities.

Acknowledgments This work was supported by National Taiwan University (R.P.C.) and the National Science Council in Taiwan (R.P.C., NSC 99-2113-M-002-002-MY2). The authors would like to thank Ms. Lin-Chen Ho for providing Fmoc-Agh(Boc)2-OH, Mr. Marc J. Koyack for the early planning stages of the project, Professor Huan-Tsung Chang (National Taiwan University) for providing us access to a fluorimeter. The authors would also like to thank Professor Cheu-Pyeng Cheng (National Tsing Hua University) for helpful discussions, and Ms. Chia-Wen Kuo for proofreading the manuscript.

Conflict of interest The authors declare that they have no conflict of interest.

References

Aharoni A, Gaidukov L, Khersonsky O, Gould SM, Roodveldt C, Tawfik DS (2005) The 'evolvability' of promiscuous protein functions. Nat Genet 37(1):73–76. doi:10.1038/Ng1482

Atherton E, Fox H, Harkiss D, Logan CJ, Sheppard RC, Williams BJ (1978) A mild procedure for solid phase peptide synthesis: use of fluorenylmethoxycarbonylamino-acids. J Chem Soc Chem Commun 13:537–539

Berman JW, Eugenin EA, King JE, Nath A, Calderon TM, Zukin RS, Bennett MVL (2007) HIV-tat induces formation of an LRP-PSD-95-NMDAR-nNOS complex that promotes apoptosis in neurons and astrocytes. Proc Natl Acad Sci USA 104(9):3438–3443. doi:10.1073/pnas.0611699104

Calnan BJ, Biancalana S, Hudson D, Frankel AD (1991a) Analysis of arginine-rich peptides from the HIV Tat protein reveals unusual features of RNA protein recognition. Gene Dev 5(2):201–210

Calnan BJ, Tidor B, Biancalana S, Hudson D, Frankel AD (1991b) Arginine-mediated RNA recognition: the arginine fork. Science 252(5009):1167–1171

Chao TY, Lavis LD, Raines RT (2010) Cellular uptake of ribonuclease a relies on anionic glycans. Biochemistry 49(50):10666–10673. doi:10.1021/Bi1013485

Cheng RP, Weng Y-J, Wang W-R, Koyack MJ, Suzuki Y, Wu C-H, Yang P-A, Hsu H-C, Kuo H-T, Girinath P, Fang C-J (2011) Helix formation and capping energetics of arginine analogs with varying side chain length. Amino Acids 43(1):195–206. doi:10.1007/s00726-011-1064-2

Choudhury I, Wang JH, Rabson AB, Stein S, Pooyan S, Stein S, Leibowitz MJ (1998) Inhibition of HIV-1 replication by a Tat RNA-binding domain peptide analog. J Acquir Immune Defic Syndr Hum Retrovirol 17(2):104–111

Cordingley MG, Lafemina RL, Callahan PL, Condra JH, Sardana VV, Graham DJ, Nguyen TM, Legrow K, Gotlib L, Schlabach AJ, Colonno RJ (1990) Sequence-specific interaction of Tat protein and Tat peptides with the transactivation-responsive sequence element of human-immunodeficiency-virus type-1 in vitro. Proc Natl Acad Sci USA 87(22):8985–8989

Cullen BR (1991) Regulation of HIV-1 gene expression. FASEB J 5(10):2361–2368

Elson-Schwab L, Garner OB, Schuksz M, Crawford BE, Esko JD, Tor Y (2007) Guanidinylated neomycin delivers large, bioactive cargo into cells through a heparan sulfate-dependent pathway. J Biol Chem 282(18):13585–13591. doi:10.1074/jbc.M700463200

Ensoli B, Buonaguro L, Barillari G, Fiorelli V, Gendelman R, Morgan RA, Wingfield P, Gallo RC (1993) Release, uptake, and effects of extracellular human-immunodeficiency-virus type-1 Tat protein on cell-growth and viral transactivation. J Virol 67(1):277–287

Gelman MA, Richter S, Cao H, Umezawa N, Gellman SH, Rana TM (2003) Selective binding of TAR RNA by a Tat-derived beta-peptide. Org Lett 5(20):3563–3565. doi:10.1021/Ol034977v

Izdebski J, Witkowska E, Kunce D, Oriowska A, Baranowska B, Wolinska-Witort E (2004) Potent trypsin-resistant hGH-RH analogues. J Pept Sci 10(8):524–529. doi:10.1002/Psc.563

Kennan AJ, Diss ML (2008) Orthogonal recognition in dimeric coiled coils via buried polar-group modulation. J Am Chem Soc 130(4):1321–1327. doi:10.1021/Ja076265w

Khersonsky O, Roodveldt C, Tawfik DS (2006) Enzyme promiscuity: evolutionary and mechanistic aspects. Curr Opin Chem Biol 10(5):498–508. doi:10.1016/j.cbpa.2006.08.011

Lakowicz JR (1999) In: Principles of fluorescence spectroscopy, 2nd edn. Kluwer Academic/Plenum Publishers, New York, pp 291–318

Levin KB, Dym O, Albeck S, Magdassi S, Keeble AH, Kleanthous C, Tawfik DS (2009) Following evolutionary paths to protein–protein interactions with high affinity and selectivity. Nat Struct Mol Biol 16(10):1049–1067. doi:10.1038/Nsmb.1670

Long KS, Crothers DM (1995) Interaction of human-immunodeficiency-virus type-1 Tat-derived peptides with TAR RNA. Biochemistry 34(27):8885–8895

McLoughlin SY, Copley SD (2008) A compromise required by gene sharing enables survival: implications for evolution of new enzyme activities. Proc Natl Acad Sci USA 105(36):13497–13502. doi:10.1073/pnas.0804804105

Mi MY, Zhang JY, He YK (2005) Inhibition of HIV derived lentiviral production by TAR RNA binding domain of TAT protein. Retrovirology 2. doi:10.1186/1742-4690-2-71

Misumi S, Takamune N, Ohtsubo Y, Waniguchi K, Shoji S (2004) Zn^{2+} binding to cysteine-rich domain of extracellular human immunodeficiency virus type 1 Tat protein is associated with Tat protein-induced apoptosis. Aids Res Hum Retrov 20(3):297–304

Mitchell DJ, Kim DT, Steinman L, Fathman CG, Rothbard JB (2000) Polyarginine enters cells more efficiently than other polycationic homopolymers. J Pept Res 56(5):318–325

Mucha P, Rekowski P, Szyk A, Kupryszewski G, Giel-Pietraszuk M, Barciszewski J (1998) Circular dichroism studies of the interaction of Tat analogues substituted in the Arg(52) position with TAR RNA HIV-1. Lett Pept Sci 5(5–6):345–348

Puglisi JD, Chen L, Blanchard S, Frankel AD (1995) Solution structure of a bovine immunodeficiency virus Tat-TAR peptide-RNA complex. Science 270(5239):1200–1203

Richard JP, Melikov K, Vives E, Ramos C, Verbeure B, Gait MJ, Chernomordik LV, Lebleu B (2003) Cell-penetrating peptides. A reevaluation of the mechanism of cellular uptake. J Biol Chem 278(1):585–590. doi:10.1074/jbc.M209548200

Ruzza P, Calderan A, Guiotto A, Osler A, Borin G (2004) Tat cell-penetrating peptide has the characteristics of a poly(proline) II helix in aqueous solution and in SDS micelles. J Pept Sci 10(7):423–426. doi:10.1002/psc.558

Soskine M, Tawfik DS (2010) Mutational effects and the evolution of new protein functions. Nat Rev Genet 11(8):572–582. doi:10.1038/Nrg2808

Stevens M, De Clercq E, Balzarini J (2006) The regulation of HIV-1 transcription: molecular targets for chemotherapeutic intervention. Med Res Rev 26(5):595–625. doi:10.1002/Med.20081

Tawfik DS (2010) Messy biology and the origins of evolutionary innovations. Nat Chem Biol 6(10):692–696. doi:10.1038/Nchembio.441

Thoren PEG, Persson D, Isakson P, Goksor M, Onfelt A, Norden B (2003) Uptake of analogs of penetratin, Tat(48–60) and oligoarginine in live cells. Biochem Biophys Res Commun 307(1):100–107. doi:10.1016/S0006-291x(03)01135-5

Vick JE, Schmidt DMZ, Gerlt JA (2005) Evolutionary potential of (beta/alpha)(8)-barrels: in vitro enhancement of a "new" reaction in the enolase superfamily. Biochemistry 44(35):11722–11729. doi:10.1021/Bi050963g

Vives E, Brodin P, Lebleu B (1997) A truncated HIV-1 Tat protein basic domain rapidly translocates through the plasma membrane and accumulates in the cell nucleus. J Biol Chem 272(25):16010–16017

Weeks KM, Ampe C, Schultz SC, Steitz TA, Crothers DM (1990) Fragments of the HIV-1 Tat protein specifically bind TAR RNA. Science 249(4974):1281–1285

Wender PA, Mitchell DJ, Pattabiraman K, Pelkey ET, Steinman L, Rothbard JB (2000) The design, synthesis, and evaluation of molecules that enable or enhance cellular uptake: peptoid molecular transporters. Proc Natl Acad Sci USA 97(24):13003–13008

Wender PA, Galliher WC, Goun EA, Jones LR, Pillow TH (2008) The design of guanidinium-rich transporters and their internalization mechanisms. Adv Drug Deliv Rev 60(4–5):452–472. doi:10.1016/j.addr.2007.10.016

Zhang JZ (2003) Evolution by gene duplication: an update. Trends Ecol Evol 18(6):292–298. doi:10.1016/S0169-5347(03)00033-8

Zondlo NJ, Schepartz A (1999) Highly specific DNA recognition by a designed miniature protein. J Am Chem Soc 121(29):6938–6939